

M. L'Hadj Said, M. Ali Moussa, T. Bessaad

Control of an autonomous wind energy conversion system based on doubly fed induction generator supplying a non-linear load

Introduction. Nowadays, many researches are being done on wind turbines providing electrical energy to a stable power grid by via a doubly fed induction generator (DFIG), but the studies on the autonomous networks are rare, due the difficulty of controlling powers often close to the nominal power of the generator. **Goal.** This paper presents a variable speed constant frequency (VSCF) autonomous control system to supply isolated loads (linear or non-linear). The main objective is the design of an effective strategy to reduce harmonic currents induced via the non-linear loads such as rectifier bridge with 6 diodes. The **novelty** of the work consists in study of system composed of a DFIG providing energy by his stator to a stand-alone grid. It uses a static converter connected to the rotor allowing operation in hypo and hyper synchronism. A permanent magnet synchronous machine (PMSM) connected to a wind turbine supplies this converter, that is sized proportionately to the variation range of the necessary rotational speed. In the case of linear loads there is no problem, all desired parameters are well controlled but in the non-linear loads case such as rectifier bridge with 6 diodes there is the harmonic problem. For this **purpose**, to reduce this harmonic, the proposed solution is the installation of a LC filter. **Methods.** The DFIG is controlled to provide a constant voltage in amplitude and frequency independently of the grid load or the drive turbine speed. This command is vector control in a reference related to the stator field. The stator flux is aligned along the d axis of this landmark allowing thus the decoupling of the active and reactive stator powers of DFIG. The DFIG is controlled by an internal control loop of rotor flux and an external control loop of output stator voltage. We present also the control of the PMSM and the DC bus of the converter. The PMSM is controlled by an internal control loop of the current and an external control loop of the continuous bus of the converter according to its nominal value. The control system of wind generator based on the maximum power point tracking and the control of bus continuous at output rectifier knowing that the non-linear loads introduce high harmonic currents and disrupt the proper functioning of the system. The installation of a LC filter between the stator and the network to be supplied reduce harmonics. **Results.** Simulation results carried out on MATLAB/Simulink show that this filter allows obtaining a quasi-sinusoidal network voltage and it also has the advantage of a simple structure, a good efficiency and a great performance. This proves the feasibility and efficiency of the proposed system for different loads (linear or non-linear). **Practical value.** This proposed system is very performing and useful compared to others because it ensures the permanent production of electricity at VSCF to feed isolated sites, whatever the load supplied (linear or non-linear), without polluting the environment so that the use of wind energy is very important to reduce the greenhouse effect. References 34, figures 9.

Key words: doubly fed induction generator, wind power, variable speed, autonomous operation, permanent magnet synchronous machine.

Вступ. В даний час проводиться багато досліджень вітряних турбін, що забезпечують електроенергією стабільну електромережу через асинхронний генератор з подвійним живленням (DFIG), але дослідження автономних мереж рідкісні через складність управління потужностями, часто близькими до номінальної потужності генератора. **Мета.** У статті представлена автономна система управління змінною швидкістю та постійною частотою (VSCF) для живлення ізольованих навантажень (лінійних чи нелінійних). Основною метою є розробка ефективної стратегії зниження гармонійних струмів, наведених через нелінійні навантаження, такі як випрямний міст із шістьма діодами. **Новизна** роботи полягає у вивченні системи, що складається з DFIG, що забезпечує енергією його статор в автономну мережу. Він використовує статичний перетворювач, підключений до ротора, що дозволяє працювати в гіпо-і гіперсинхронізмі. Синхронна машина з постійними магнітами (PMSM), підключена до вітряної турбіни, живить цей перетворювач, який має розмір, пропорційний діапазону зміни необхідної швидкості обертання. У разі лінійних навантажень проблем немає, всі бажані параметри добре контролюються, але у разі нелінійних навантажень, таких як випрямний міст із шістьма діодами, виникає проблема гармонік. Для цієї мети, щоб зменшити цю гармоніку, запропонованим рішенням є встановлення LC-фільтру. **Методи.** DFIG управляється для забезпечення постійної напруги за амплітудою та частотою незалежно від навантаження мережі або швидкості приводної турбіни. Ця команда є векторним управлінням в опорному сигналі, пов'язаному з полем статора. Потік статора вирівняний вздовж осі d цього орієнтуру, що дозволяє таким чином розв'язати активну та реактивну потужності статора DFIG. DFIG управляється внутрішнім контуром управління потоком ротора та зовнішнім контуром управління вихідною напругою статора. Представлено також управління PMSM та DC шиною перетворювача. PMSM управляється внутрішнім контуром керування струмом та зовнішнім контуром керування безперервною шиною перетворювача відповідно до його номінального значення. Система керування вітрогенератором базується на відстеженні точки максимальної потужності та безперервному керуванні шиною на вихідному випрямлячі, враховуючи, що нелінійні навантаження вводять струми високих гармонік та порушують належне функціонування системи. Встановлення LC-фільтра між статором і мережею живлення зменшує гармоніки. **Результати** моделювання, проведені в MATLAB/Simulink, показують, що цей фільтр дозволяє отримати квазісинусоїдальну напругу мережі, а також має перевагу щодо простоти структури, хорошої ефективності та значної продуктивності. Це доводить доцільність та ефективність запропонованої системи для різних навантажень (лінійних чи нелінійних). **Практична значимість.** Запропонована система дуже продуктивна і корисна в порівнянні з іншими, оскільки вона забезпечує постійне виробництво електроенергії на VSCF для живлення ізольованих ділянок, незалежно від навантаження, що подається (лінійне або нелінійне), не забруднюючи навколишнє середовище, тому що використовує енергію вітру, що є важливим для зниження парникового ефекту. Бібл. 34, рис. 9.

Ключові слова: асинхронний генератор з подвійним живленням, вітроенергетика, змінна швидкість, автономна робота, синхронна машина з постійними магнітами.

Introduction. Electrical energy and electrical power systems frameworks play essential roles in the economic development of a country [1, 2]. Sustainable development and renewable energies arouse the interest of several research teams. The use of wind energy and renewable

sources is essential to reduce the greenhouse effect [3]. Thus, the development of wind turbines represents a great investment in technological research [4]. These systems which produce electrical energy from the wind can

© M. L'Hadj Said, M. Ali Moussa, T. Bessaad

constitute a technological and economical alternative to the various exhaustible energy sources [5–7]. Wind turbines are believed to be a potential source of electrical energy in the near future [8, 9]. Wind turbines undergo both cycles, i.e. coercion and change in wind behavior [8–10].

A large part of the wind turbines use the asynchronous machines with double power. The utilization the doubly fed induction generator (DFIG) as a generation unit in the wind generation structures has been granted great concern during the past and present decades [11–14]. The superiority of the DFIG over other generation units comes from its ability to handle higher power ratings compared with the other units. Due to the physical construction of the DFIG, it has the ability to be controlled from both the grid and rotor sides [15]. The possibility of performing the control from the rotor side has enabled the utilization of low power inverters, which resulted in saving the cost [16, 17]. This generator allows the production of electricity at variable speed [18–23]. It gives the opportunity, then, to better control wind resources for different wind conditions [21–23].

Nowadays, many researches are being done on wind turbines providing electrical energy to a stable power grid by via a DFIG, but the studies on the autonomous networks are rare, due the difficulty of controlling powers often close to the nominal power of the generator.

The following work shows firstly, the control strategy of a DFIG, providing energy by the stator to an autonomous grid. It uses a static converter connected to the rotor allowing operation in hypo and hyper synchronism. A permanent magnet synchronous machine (PMSM) connected to a wind turbine feeds this converter (Fig. 1), that is sized proportionately to the variation range of the necessary rotational speed [24].

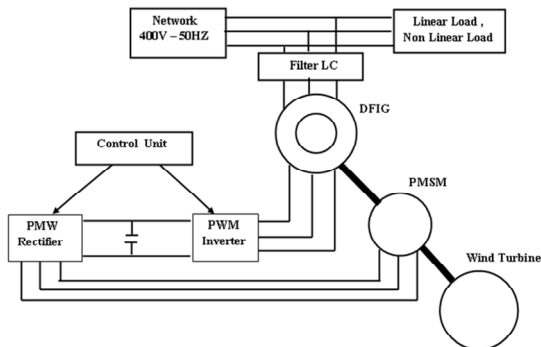


Fig 1. Global schema of the proposed system

The DFIG is controlled to provide a constant voltage in amplitude and frequency independently of the grid load or the drive turbine speed. This command is vector control in a reference related to the stator field. The stator flux is aligned along the d axis of this landmark allowing thus the decoupling of the active and reactive stator powers of DFIG [25–27].

The control strategy is carried out in two loops: an internal control loop of the rotor flux and an external control loop of the stator voltage. We have also; the PMSM is controlled by an internal control loop of the current and an external control loop of the continuous bus of the converter according to its nominal value [28].

The **aim** of this work is the improve the performance of this proposed system to feed isolated sites at variable

speed constant frequency (VSCF), whatever the load desired to supply it, especially the non-linear loads. In the case of linear loads there is no problem, all desired parameters are well controlled but in the non-linear loads case such as the rectifier bridge with 6 diodes there is the harmonic problem.

These loads introduce high harmonic currents and disrupt the proper functioning of the system. The solution proposed to reduce harmonics is the installation of an LC filter between the stator and the network to be supplied. This filter allows obtaining a quasi-sinusoidal network voltage and it also has the advantage of a simple structure, a good efficiency and a great performance.

The control system of wind generator is based on the maximum power point tracking (MPPT) and the control of bus continuous at output rectifier. A power maximization algorithm determines the speed of the turbine that achieves maximum power generated, by estimating the speed of the wind corresponding to the optimal advance factor [29–31].

DFIG model. The equations of DFIG in d - q axis are [32]:

$$V_{sd} = R_s i_{sd} + \frac{d\phi_{sd}}{dt} - \omega_s \phi_{sq}; \quad (1)$$

$$V_{sq} = R_s i_{sq} + \frac{d\phi_{sq}}{dt} - \omega_s \phi_{sd}; \quad (2)$$

$$V_{rd} = R_r i_{rd} + \frac{d\phi_{rd}}{dt} - (\omega_s - \omega_r) \phi_{rq}; \quad (3)$$

$$V_{rq} = R_r i_{rq} + \frac{d\phi_{rq}}{dt} - (\omega_s - \omega_r) \phi_{rd}; \quad (4)$$

$$\phi_{sd} = L_s i_{sd} + M i_{rd}; \quad (5)$$

$$\phi_{sq} = L_s i_{sq} + M i_{rq}; \quad (6)$$

$$\phi_{rd} = L_r i_{rd} + M i_{sd}; \quad (7)$$

$$\phi_{rq} = L_r i_{rq} + M i_{sq}; \quad (8)$$

where V_s , V_r , R_s , R_r , i_s , i_r , ϕ_s , ϕ_r , L_s , L_r are the voltages, resistances, currents, fluxes and inductances of the stator and rotor, respectively; M is the mutual inductance; ω_s is the synchronous speed; ω_r is the rotor speed.

The reference related to the stator field is chosen. The stator flux is aligned with the axis d of this reference which corresponds to the following equations:

$$\phi_{sq} = 0, \quad \frac{d\phi_{sd}}{dt} = 0. \quad (9)$$

In order to present the principles of this command, we neglect the resistances of stator and assume that the permanent state is reached. The voltage is therefore fixe in amplitude and frequency, we obtain the follow relation:

$$\begin{cases} V_{sd} \approx \frac{d\phi_{sd}}{dt} \approx 0; \\ V_{sq} \approx \omega_s \phi_{sd} \approx V_s. \end{cases} \quad (10)$$

From (5), (6), (9), σ is the DFIG scattering coefficient, the constraint (11) corresponds to the good orientation of the landmark chosen:

$$i_{rq} = -\frac{L_s}{M} i_{sq} \Leftrightarrow \phi_{rq} = -\frac{\sigma L_s L_r}{M} i_{sq}. \quad (11)$$

From (8), (10), (11), the new expression of active and reactive power became:

Model of PMSM. The model of PMSM is given by the system (21) using Park method in a reference frame linked to its rotating field:

$$\begin{cases} V_d = R_{ms}I_d + L_d \frac{dI_d}{dt} - E_{md}; \\ V_q = R_{ms}I_q + L_q \frac{dI_q}{dt} - E_{mq}; \end{cases} \quad (21)$$

$$\begin{cases} E_{md} = -\omega L_q I_q; \\ E_{mq} = -\omega L_d I_d - \omega \Phi_a, \end{cases} \quad (22)$$

where E_{md} , E_{mq} are the coupling terms; R_{ms} is the stator resistance; L_d , L_q are the direct and quadrature inductances; V_d , V_q , I_d , I_q are the components d - q stator voltages and currents; Φ_a is the flux of the permanent magnet; $\omega = p\Omega$ is the voltage pulsation; Ω is the speed of rotation; p is the number of pairs of poles.

The voltages being input variables, we can express the output variables (current) as follows:

$$\begin{cases} \frac{dI_d}{dt} = \frac{1}{L_d} (V_d - R_{ms}I_d + \omega L_q I_q); \\ \frac{dI_q}{dt} = \frac{1}{L_d} (V_q - R_{ms}I_q - \omega L_d I_d - \omega \Phi_a) \end{cases} \quad (23)$$

Knowing that in our case $L_d = L_q = L$.

Control of wind generator. The block control of wind generator diagram is shown in Fig. 2. The control system based on two functions: MPPT and the control of bus continuous at output rectifier.

Power maximization strategy. The equations of electric and mechanical powers of the system in permanent regime allow to new the formulation of the new objective. However, the function of mechanical power, a simpler form is used. To reduce the degrees of freedom of the system, wind speed, only uncontrollable variable of the system, is out of the mathematical formulation by the use of an optimal form [33, 34].

The equation of the wind power P_w corresponding to a wind speed V_v is given as:

$$P_w = C_p(\lambda) \frac{\rho S V_v^3}{2}, \quad (24)$$

where C_p is the power coefficient; λ is the tip-speed ratio; ρ is the air density; S is the blade surface.

If the tip-speed ratio λ is maintained at its optimal λ_{opt} value, the power coefficient is always at its maximum value $C_{pmax} = C_p(\lambda_{opt})$.

Therefore, the power of wind is also at its maximum value:

$$P_w^{opt} = C_{pmax} \frac{\rho S V_v^3}{2}. \quad (25)$$

On the other hand, if the equation of assumed tip-speed ratio maintained at the optimal value, we isolate the wind speed (26) for replacing in the equation of the maximum mechanical power (25), we obtain the (27):

$$\lambda^{opt} = \frac{\Omega R}{V_v} \Rightarrow V_v = \frac{\Omega R}{\lambda^{opt}}; \quad (26)$$

$$P_w^{opt} = \frac{1}{2} C_{pmax} \rho S \left(\frac{R}{\lambda^{opt}} \right)^3 \Omega^3. \quad (27)$$

We obtain an analytical form of the maximum mechanical power of the wind turbine depending to its speed of rotation Ω only. Considering that the conditions are optimal (at optimum power) then the (27) allows the calculation of the value of the optimum torque:

$$T_w^{opt} = \frac{1}{2} C_{pmax} \rho S \left(\frac{R}{\lambda^{opt}} \right)^3 \Omega^2. \quad (28)$$

Regulation of the stator current of the PMSM. The transfer functions between the voltages and currents of the PMSM are first order and are regulated by PI correctors as shown in the block diagram on Fig. 3. The transfer function of the machine being of the form:

$$H(s) = \frac{I_{dq}(s)}{V_{dq}(s) + E_{mdq}(s)}; \quad (29)$$

$$H(s) = \frac{1}{E_{ms} + L_{dq}(s)} = \frac{1/R_{ms}}{1 + \frac{L_{dq}}{R_{ms}} s}. \quad (30)$$

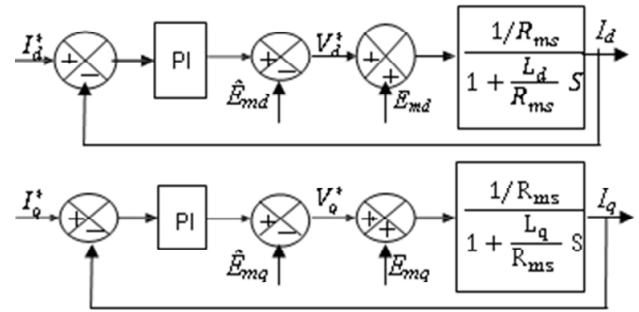


Fig. 3. Regulation loop of current of the PMSM

In permanent regime and neglecting the stator resistance, the equations (21), (22) give the following system:

$$\begin{cases} V_d = -\omega L_q I_q; \\ V_q = \omega L_d I_d + \omega \Phi_a. \end{cases} \quad (31)$$

Furthermore, neglecting the losses introduced by the converter, we can write:

$$P_{dc} = V_d I_d + V_q I_q = V_{dc} I_{dc}, \quad (32)$$

where P_{dc} is the active power; V_{dc} is the continuous bus voltage; I_{dc} is the output current of the rectifier.

With the help of (31), (32) we obtain:

$$I_q^* = P_{dc} / \omega \Phi_a, \quad (33)$$

$$V_d = P_{dc} L_q / \Phi_a. \quad (34)$$

The relations (33), (34) show that the components of the direct voltage and the quadrature current depend to the desired rotor power. A conventional method controlling of the motor starting asynchronous power (MSAP) seeking to obtain maximum power for a minimum of current. However if $I_{dref}=0$ the stator voltage is given by (35). This voltage is acceptable as long as it is below the limit voltage V_{lim} fixed by the continuous bus voltage (36):

$$|V| = \sqrt{\left(\frac{P L_q}{\Phi_a} \right)^2 + (\omega \Phi_a)^2}; \quad (35)$$

$$|V| < V_{lim}. \quad (36)$$

Control loop of the continuous voltage V_{dc}
According to (32), (33) the equation of the power is:

$$P_{dc} = \omega \Phi_a I_q = V_{dc} I_{dc} \Rightarrow I_q = \frac{V_{dc}}{\omega \Phi_a} I_{dc} \quad (37)$$

Figure 3 allows us to write:

$$I_{dc} = I_c + I_L \quad (38)$$

Supposing that the losses are null

$$C \frac{dV_{dc}}{dt} = I_{dc} - I_L \quad (39)$$

The block diagram of this loop is shown in Fig. 4. The regulation is done with PI correctors after setting the damping factor and the natural frequency desired.

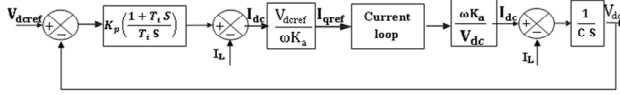
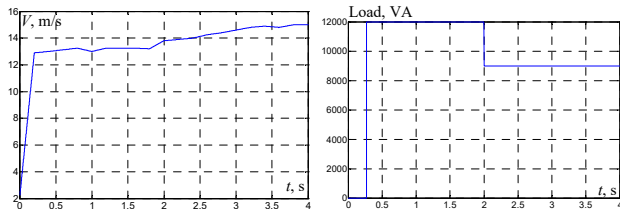


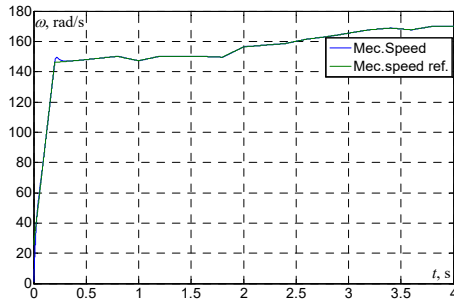
Fig. 4. Regulation of the continuous bus voltage

Simulation results. Linear load case. The proposed system has been tested in MATLAB / Simulink using the electrical parameters of the DFIG and PMSM, the reference voltage at the rectifier output being taken equal to 150 V, it is assumed that this DFIG and MSAP are driven by a wind turbine, wind speed is variable in time to feed a load RL. Load whose power consumption is expected to vary according to the following time table: 0 kVA at time $t = 0$ s, 12 kVA at $t = 0.5$ s and 9 kVA at time $t = 2$ s with 0.8 power factor. The obtained simulation results (Fig. 5) prove the feasibility of the proposed system for the maximum load variable power in the time. The values also show that the stator voltage V_s and the continuous voltage V_{dc} are entirely controlled during the variation of the load and wind speed. This therefore proves the feasibility of the system in hypo and hyper synchronism.

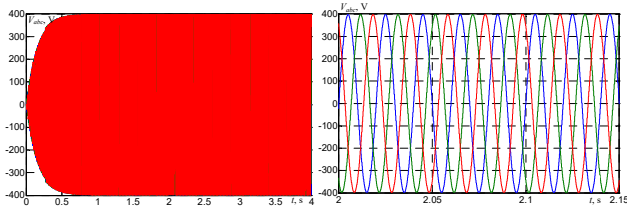


a) wind speed

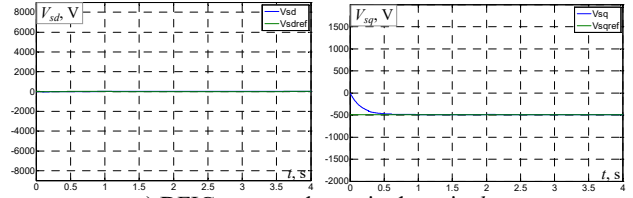
b) load



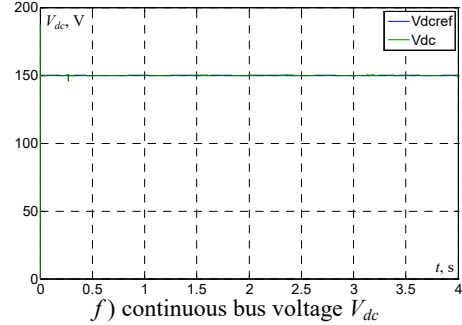
c) mechanical speed



d) stator voltage generated by the DFIG with zoom



e) DFIG stator voltages in the axis d - q



f) continuous bus voltage V_{dc}

Fig. 5. Simulation results of the proposed system for linear load

Non-linear load case. After having studied the functioning of the DFIG on linear load, we will study the performance of the latter on a non-linear load made up of a converter (rectifier bridges with 6 diodes) which supplies an inductive load (see Fig. 6):

$$I_d = U_d / (L_s + R) \quad (40)$$

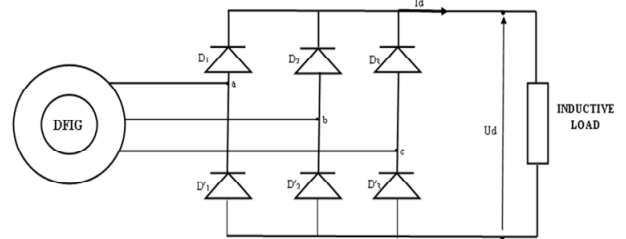


Fig. 6. Structure of a 6-pulse diode rectifier

The rectified voltage is obtained by:

$$U_d = V_{js \max} - V_{js \min} \quad (41)$$

Inserting a 6-diode rectifier bridge into the system does not change the test procedure; the only difference is the introduction of non-linear loads instead of linear RL loads. Indeed, this type of converter induces a large number of current harmonics:

$$\begin{cases} I_{sf} = \sqrt{3} I_d / \pi; & I_{sh} = I_{sf} / h; \\ h = 6n \pm 1; & THD_{I_s} = \sqrt{\sum I_{sh}^2} / I_{sf}, \end{cases} \quad (42)$$

where I_{sf} is the amplitude of the fundamental current; I_{sh} is the harmonic current of order h ; I_d is the continue current flowing through the load; THD_{I_s} is the total harmonic distortion of the load current.

The simulation results clearly show the deterioration of the stator voltage due to the induced harmonic currents caused by the load currents. The more the load increases the load current becomes more and more distorting. The active and reactive powers are also deteriorated by this non-linear load due to the harmonics induced by the 6-diode rectifier bridge. These harmonics increase the losses in the DFIG and promote excessive heating of the latter. The simulation results are shown in Fig. 7.

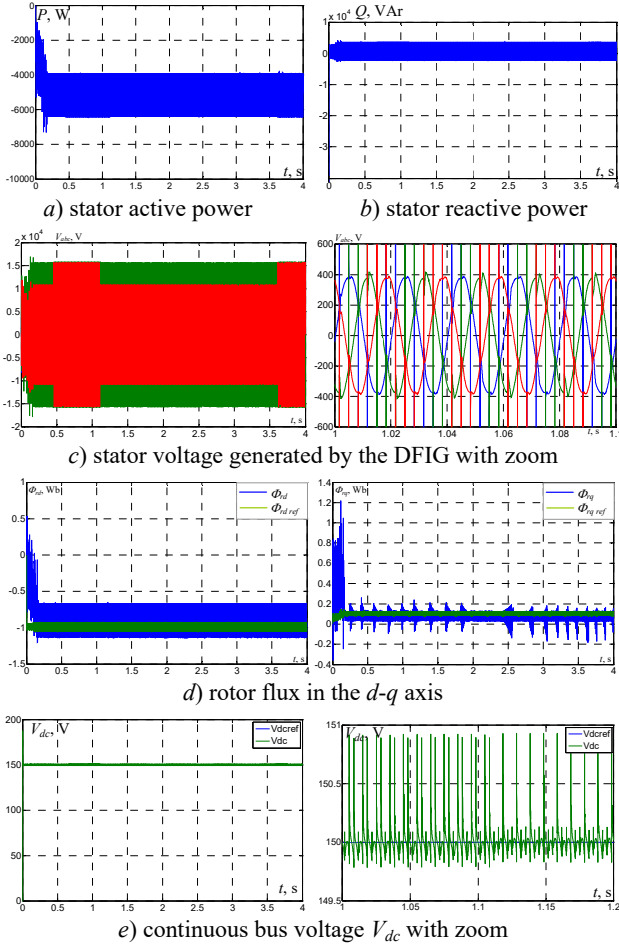


Fig. 7. Simulation results of the proposed system for non-linear load

Filtering characteristics. LC filter is placed on the stator side of the DFIG to eliminate voltage harmonics from the on-board network. The single-phase equivalent model of the filter is given in Fig. 8.

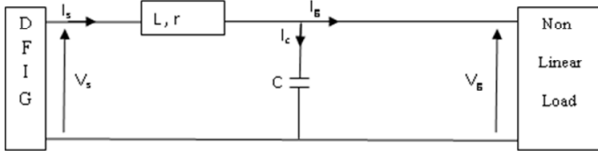


Fig 8. Single-phase equivalent diagram of the LC filter

This filter can be represented by the following equation of state:

$$\frac{d}{dt} \begin{bmatrix} I_s \\ V_g \end{bmatrix} = \begin{bmatrix} -\frac{r}{L} & -\frac{1}{L} \\ \frac{1}{C} & 0 \end{bmatrix} \begin{bmatrix} I_s \\ V_g \end{bmatrix} + \begin{bmatrix} 0 & \frac{1}{L} \\ -\frac{1}{C} & 0 \end{bmatrix} \begin{bmatrix} I_g \\ V_s \end{bmatrix}, \quad (43)$$

where L , r are the filter inductance and its internal resistance; C is the filter capacitance; V_s , I_s , I_g , V_g are respectively the stator voltage and current of the DFIG, and the current and voltage of the non-linear load. V_s can be considered as the filter input variable, I_g – the disturbance variable and V_g – the filter output variable. From (43), we can write 4 transfer functions to describe the operation of the filter:

$$\begin{bmatrix} I_s(s) \\ V_g(s) \end{bmatrix} = \frac{\omega_0^2}{s^2 + 2m\omega_0 s + \omega_0^2} \begin{bmatrix} 1 & Cs \\ Ls + r & 1 \end{bmatrix} \begin{bmatrix} I_g(s) \\ V_s(s) \end{bmatrix}, \quad (44)$$

where $\omega_0 = 1/\sqrt{LC}$ is the resonance frequency; m is the damping coefficient.

This presentation shows that the load current harmonics due to the 6-diode rectifier bridge deteriorate the stator current as well as the load voltage vector. The filter parameters must therefore be chosen so as to reduce the harmonic distortion rate of the mains voltage to a value less than 5%. We can derive from (44) the transfer function between $I_g(s)$ and $V_g(s)$:

$$\frac{V_g(s)}{I_g(s)} = \frac{(Ls + r)\omega_0^2}{s^2 + 2m\omega_0 s + \omega_0^2}. \quad (45)$$

Design procedure. The filter inductance is typically sized equal to a fraction of the rated motor impedance, so voltage drop is reduced across the filter inductance. In this case, we will choose:

$$L = 0.7 \cdot L_s. \quad (46)$$

The resistance in this case corresponds to the internal resistance of the inductance and thus is proportional to the internal Joule losses of the inductance. This resistance creates losses at the level of the filter. In this case, the Joule losses are defined to be less than 1% of the total power, so the maximum acceptable internal resistance r_{\max} can be calculated as:

$$r_{\max} = \frac{0.01 P_{s-nom}}{3 I_{s-nom}^2}. \quad (47)$$

The attenuation provided by the filter depends on the damping coefficient m . The cutoff frequency should be low enough to give the desired attenuation and the damping coefficient large enough to increase that attenuation. On the other hand, (44) shows that a low cutoff frequency may result in large components value and size. In addition, a very large damping coefficient would result in an internal resistance value more important than r_{\max} . It is therefore necessary to find a compromise between the dimensions of the filter and the desired THD.

From the components of the harmonic current described by (42), the amplitude-frequency characteristics given by (45) and knowing that the amplitude of the voltage of the fundamental is 400 V, we can calculate the relationship between the filter cutoff frequency and the THD of the mains voltage after filtering.

Finally, knowing ω_0 and L , we can deduce the capacity of the filter:

$$C = 1/L\omega_0^2. \quad (48)$$

The introduction of an LC filter with a cutoff frequency of 816.5 rad/s with a damping coefficient $m=0.734$ to reduce current harmonics is simulated in the same way as before.

The simulation results (Fig. 9) show that the load voltage is almost sinusoidal for a non-linear load. Compared to the signal obtained without a filter, the oscillations on the active and reactive power are greatly reduced by the introduction of the filter. These simulations carried out on MATLAB/Simlink prove the efficiency of the proposed system in the event of non-linear loads.

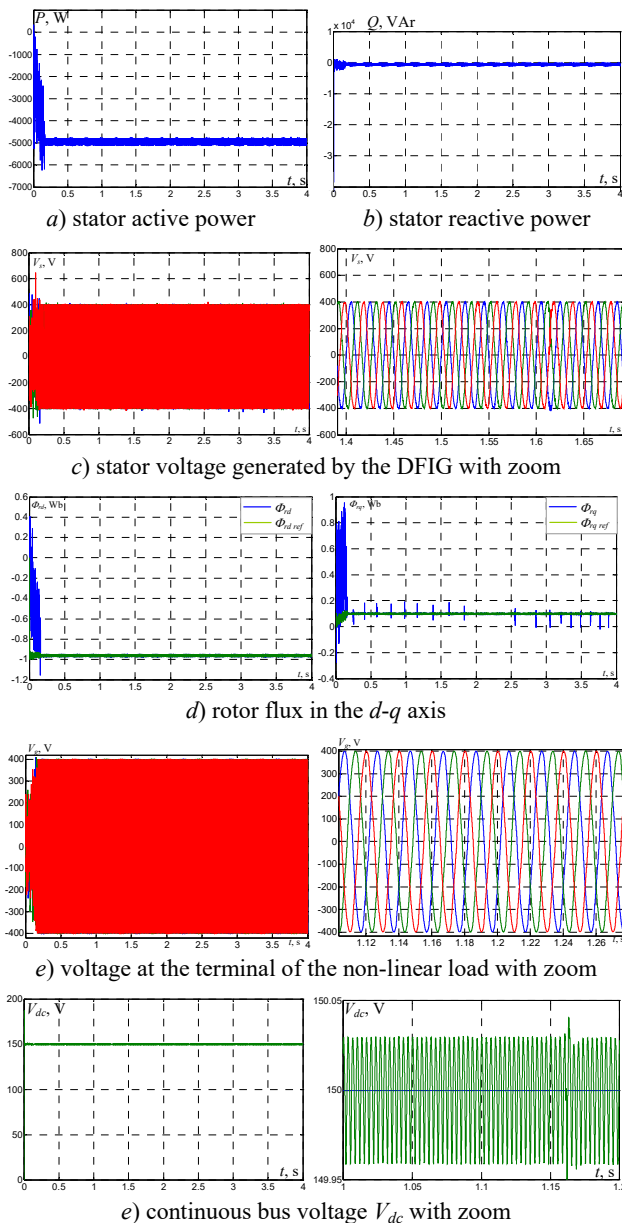


Fig 9. Simulation results of the proposed system for non-linear load after the introduction of LC filter

Conclusions.

This paper has enabled us to study an autonomous electrical generation system working at variable speed and fixed frequency to supply isolated loads. The principles of vector control of DFIG and PMSM have been presented. The simulation results carried out on MATLAB/Simulink show that this method makes it possible to obtain a voltage at fixed frequency and amplitude under a wide range of variation of the turbine drive speed. The addition of non-linear loads, such as diode rectifier bridges, introduces harmonics which deteriorate the voltages of the network. The introduction of an LC filter on the stator side of the DFIG allows these harmonics to be reduced to an acceptable level. This proves the efficiency of the proposed system for different loads (linear and non-linear loads).

Conflict of interest. The authors declare that they have no conflicts of interest.

REFERENCES

1. Strielkowski W., Civiñ L., Tarkhanova E., Tvaronavičienė M., Petrenko Y. Renewable Energy in the Sustainable Development of Electrical Power Sector: A Review. *Energies*, 2021, vol. 14, no. 24, art. no. 8240. doi: <https://doi.org/10.3390/en14248240>.
2. Duong M., Leva S., Mussetta M., Le K. A Comparative Study on Controllers for Improving Transient Stability of DFIG Wind Turbines During Large Disturbances. *Energies*, 2018, vol. 11, no. 3, art. no. 480. doi: <https://doi.org/10.3390/en11030480>.
3. Benbouhenni H., Lemdani S. Combining synergetic control and super twisting algorithm to reduce the active power undulations of doubly fed induction generator for dual-rotor wind turbine system. *Electrical Engineering & Electromechanics*, 2021, no. 3, pp. 8-17. doi: <https://doi.org/10.20998/2074-272X.2021.3.02>.
4. Ouerghi F.H., Omri M., Menaem A.A., Taloba A.I., Abd El-Aziz R.M. Feasibility evaluation of wind energy as a sustainable energy resource. *Alexandria Engineering Journal*, 2024, vol. 106, pp. 227-239. doi: <https://doi.org/10.1016/j.aej.2024.06.055>.
5. Shanu S., Barath Raj R.K., Thampatty K.C.S. Wind Resource Assessment and Techno-economic Analysis using WaSP software – A Case Study. *2023 IEEE Technology & Engineering Management Conference - Asia Pacific (TEMSCON-ASPAC)*, 2023, pp. 1-7. doi: <https://doi.org/10.1109/TEMSCON-ASPAC59527.2023.10531485>.
6. Evans L.E., Dolšak N., Prakash A. Do windy areas have more wind turbines: An empirical analysis of wind installed capacity in Native tribal nations. *PLOS ONE*, 2022, vol. 17, no. 2, art. no. e0261752. doi: <https://doi.org/10.1371/journal.pone.0261752>.
7. Muthukaruppasamy S., Dharmaprakash R., Sendilkumar S., Parimalasundar E. Enhancing off-grid wind energy systems with controlled inverter integration for improved power quality. *Electrical Engineering & Electromechanics*, 2024, no. 5, pp. 41-47. doi: <https://doi.org/10.20998/2074-272X.2024.5.06>.
8. Nejad A.R., Keller J., Guo Y. et al. Wind turbine drivetrains: state-of-the-art technologies and future development trends. *Wind Energy Science*, 2022, vol. 7, no. 1, pp. 387-411. doi: <https://doi.org/10.5194/wes-7-387-2022>.
9. Ahmed S.D., Al-Ismail F.S.M., Shafulh M., Al-Sulaiman F.A., El-Amin I.M. Grid Integration Challenges of Wind Energy: A Review. *IEEE Access*, 2020, vol. 8, pp. 10857-10878. doi: <https://doi.org/10.1109/ACCESS.2020.2964896>.
10. Berhanu Tuka M., Leidhold R., Mamo M. Modeling and control of a Doubly Fed Induction Generator using a back-to-back converters in grid tied wind power system. *2017 IEEE PES PowerAfrica*, 2017, pp. 75-80. doi: <https://doi.org/10.1109/PowerAfrica.2017.7991202>.
11. El Mouden A., Hmidat A., Aarib A. Comparison of the active and reactive powers of the asynchronous cage machine and the doubly fed induction generator used in wind turbine energy in the case of decentralized production on an isolated site. *International Journal on Electrical Engineering and Informatics*, 2023, vol. 15, no. 1, pp. 50-63. doi: <https://doi.org/10.15676/ijeei.2023.15.1.4>.
12. Abdeen M., Li H., Kamel S., Khaled A., El-Dabah M., Kharrich M., Sindi H.F. A Recent Analytical Approach for Analysis of Sub-Synchronous Resonance in Doubly-Fed Induction Generator-Based Wind Farm. *IEEE Access*, 2021, vol. 9, pp. 68888-68897. doi: <https://doi.org/10.1109/ACCESS.2021.3075965>.
13. Chhipa A.A., Chakrabarti P., Bolshev V., Chakrabarti T., Samarín G., Vasilyev A.N., Ghosh S., Kudryavtsev A. Modeling and Control Strategy of Wind Energy Conversion System with Grid-Connected Doubly-Fed Induction Generator. *Energies*, 2022, vol. 15, no. 18, art. no. 6694. doi: <https://doi.org/10.3390/en15186694>.
14. Marques G.D., Iacchetti M.F. DFIG Topologies for DC Networks: A Review on Control and Design Features. *IEEE Transactions on Power Electronics*, 2019, vol. 34, no. 2, pp. 1299-1316. doi: <https://doi.org/10.1109/TPEL.2018.2829546>.

15. Mossa M.A., Duc Do T., Saad Al-Sumaiti A., Quynh N.V., Diab A.A.Z. Effective Model Predictive Voltage Control for a Sensorless Doubly Fed Induction Generator. *IEEE Canadian Journal of Electrical and Computer Engineering*, 2021, vol. 44, no. 1, pp. 50-64. doi: <https://doi.org/10.1109/ICJECE.2020.3018495>.
16. Wei X., Cheng M., Wang W., Han P., Luo R. Direct Voltage Control of Dual-Stator Brushless Doubly Fed Induction Generator for Stand-Alone Wind Energy Conversion Systems. *IEEE Transactions on Magnetics*, 2016, vol. 52, no. 7, pp. 1-4. doi: <https://doi.org/10.1109/TMAG.2016.2526049>.
17. Bebars A.D., Eladl A.A., Abdulsalam G.M., Badran E.A. Internal electrical fault detection techniques in DFIG-based wind turbines: a review. *Protection and Control of Modern Power Systems*, 2022, vol. 7, no. 1, art. no. 18. doi: <https://doi.org/10.1186/s41601-022-00236-z>.
18. Zhang Y., Jiang T. Robust Predictive Stator Current Control Based on Prediction Error Compensation for a Doubly Fed Induction Generator Under Nonideal Grids. *IEEE Transactions on Industrial Electronics*, 2022, vol. 69, no. 5, pp. 4398-4408. doi: <https://doi.org/10.1109/TIE.2021.3080200>.
19. Din Z., Zhang J., Xu Z., Zhang Y., Zhao J. Low voltage and high voltage ride-through technologies for doubly fed induction generator system: Comprehensive review and future trends. *IET Renewable Power Generation*, 2021, vol. 15, no. 3, pp. 614-630. doi: <https://doi.org/10.1049/rpg2.12047>.
20. Metwally M.M., Ratib M.K., Aly M.M., Abdel-Rahim A.M. Effect of Grid Faults on Dominant Wind Generators for Electric Power System Integration: A Comparison and Assessment. *Energy Systems Research*, 2021, vol. 3, no. 15, pp. 70-78. doi: <https://doi.org/10.38028/esr.2021.03.0007>.
21. Beniss M.A., El Moussaoui H., Lamhamdi T., El Markhi H. Performance analysis and enhancement of direct power control of DFIG based wind system. *International Journal of Power Electronics and Drive Systems (IJPEDS)*, 2021, vol. 12, no. 2, pp. 1034-1044. doi: <https://doi.org/10.11591/ijpeds.v12.i2.pp1034-1044>.
22. Dannier A., Fedele E., Spina I., Brando G. Doubly-Fed Induction Generator (DFIG) in Connected or Weak Grids for Turbine-Based Wind Energy Conversion System. *Energies*, 2022, vol. 15, no. 17, art. no. 6402. doi: <https://doi.org/10.3390/en15176402>.
23. Ansari A.A., Dyanamina G. Fault Ride-Through Operation Analysis of Doubly Fed Induction Generator-Based Wind Energy Conversion Systems: A Comparative Review. *Energies*, 2022, vol. 15, no. 21, art. no. 8026. doi: <https://doi.org/10.3390/en15218026>.
24. Cardenas R., Pena R., Alepuz S., Asher G. Overview of Control Systems for the Operation of DFIGs in Wind Energy Applications. *IEEE Transactions on Industrial Electronics*, 2013, vol. 60, no. 7, pp. 2776-2798. doi: <https://doi.org/10.1109/TIE.2013.2243372>.
25. Xiao H., Zhao Z., Zhou K., Guo J., Lai C.S., Lei Lai L. Voltage-Source Control of DFIG in Standalone Wind Power-Based Microgrids. *2020 IEEE 1st China International Youth Conference on Electrical Engineering (CIYCEE)*, 2020, pp. 1-7. doi: <https://doi.org/10.1109/CIYCEE49808.2020.9332674>.
26. Hamid B., Hussain I., Iqbal S.J., Singh B., Das S., Kumar N. Optimal MPPT and BES Control for Grid-Tied DFIG-Based Wind Energy Conversion System. *IEEE Transactions on Industry Applications*, 2022, vol. 58, no. 6, pp. 7966-7977. doi: <https://doi.org/10.1109/TIA.2022.3202757>.
27. Smay Y., Touaiti B., Jemli M., Ben Azza H. Experimental implementation of voltage and frequency regulation in DFIG connected to a DC-link for marine current energy conversion system. *Electrical Engineering*, 2022, vol. 104, no. 4, pp. 2355-2367. doi: <https://doi.org/10.1007/s00202-021-01485-1>.
28. Said M.L., Moulahoum S., Bounekhla M., Kabache N., Houassine H. Autonomous operation of a doubly fed induction generator driven by a wind turbine. *2015 20th International Conference on Methods and Models in Automation and Robotics (MMAR)*, 2015, pp. 1050-1055. doi: <https://doi.org/10.1109/MMAR.2015.7284024>.
29. Shutari H., Ibrahim T., Mohd Nor N.B., Saad N., Tajuddin M.F.N., Abdulrab H.Q.A. Development of a Novel Efficient Maximum Power Extraction Technique for Grid-Tied VSWT System. *IEEE Access*, 2022, vol. 10, pp. 101922-101935. doi: <https://doi.org/10.1109/ACCESS.2022.3208583>.
30. Hammoudi B.A., Serhoud H. The wind turbine's direct power control of the doubly-fed induction generator. *International Journal of Power Electronics and Drive Systems (IJPEDS)*, 2024, vol. 15, no. 2, pp. 1201-1210. doi: <https://doi.org/10.11591/ijpeds.v15.i2.pp1201-1210>.
31. Mahgoun M.S., Badoud A.E. New design and comparative study via two techniques for wind energy conversion system. *Electrical Engineering & Electromechanics*, 2021, no. 3, pp. 18-24. doi: <https://doi.org/10.20998/2074-272X.2021.3.03>.
32. Forchetti D., Garcia G., Valla M.I. Vector control strategy for a doubly-fed stand-alone induction generator. *IEEE 2002 28th Annual Conference of the Industrial Electronics Society. IECON 02*, 2002, vol. 2, pp. 991-995. doi: <https://doi.org/10.1109/IECON.2002.1185407>.
33. Mirecki A., Roboam X., Richardeau F. Architecture Complexity and Energy Efficiency of Small Wind Turbines. *IEEE Transactions on Industrial Electronics*, 2007, vol. 54, no. 1, pp. 660-670. doi: <https://doi.org/10.1109/TIE.2006.885456>.
34. Knight A.M., Peters G.E. Simple Wind Energy Controller for an Expanded Operating Range. *IEEE Transactions on Energy Conversion*, 2005, vol. 20, no. 2, pp. 459-466. doi: <https://doi.org/10.1109/TEC.2005.847995>.

Received 14.12.2024
Accepted 27.01.2025
Published 02.07.2025

M. L'Hadj Said¹, Doctoral Student,
M. Ali Moussa¹, Associate Professor,
T. Bessaad¹, Associate Professor,
Laboratory LGEER, Department of Electrotechnic,
University of Hassiba BenBouali, Chlef, Algeria,
e-mail: m.lhadjsaid@univ-chlef.dz (Corresponding Author);
m.alimoussa@univ-chlef.dz; t.bessaad@univ-chlef.dz

How to cite this article:

L'Hadj Said M., Ali Moussa M., Bessaad T. Control of an autonomous wind energy conversion system based on doubly fed induction generator supplying a non-linear load. *Electrical Engineering & Electromechanics*, 2025, no. 4, pp. 3-10. doi: <https://doi.org/10.20998/2074-272X.2025.4.01>